ISSN 2070-0482, Mathematical Models and Computer Simulations, 2018, Vol. 10, No. 2, pp. 255–264. © Pleiades Publishing, Ltd., 2018.
Original Russian Text © V.V. Kuzenov, S.V. Ryzhkov, 2017, published in Matematicheskoe Modelirovanie, 2017, Vol. 29, No. 9, pp. 19–32.

Numerical Modeling of Laser Target Compression in an External Magnetic Field

V. V. Kuzenov[a, b, *] and S. V. Ryzhkov[a, **]

[a] *Bauman Moscow State Technical University, Moscow, Russia*

[b] *Ishlinsky Institute for Problems in Mechanics, Russian Academy of Sciences, Moscow, Russia*

**e-mail: vik.kuzenov@gmail.com*

***e-mail: svryzhkov@bmstu.ru*

Received May 25, 2016

Abstract—A mathematical model for the compression process of a cylindrically symmetric thermonuclear target is presented. A numerical method of an increased accuracy order is considered, which is used to calculate the basic physical processes that occur in target plasma exposed to an external magnetic field.

Keywords: magnetic confinement fusion, laser driver, inhomogeneous electric and magnetic fields, magnetized plasma, development of numerical methods

DOI: 10.1134/S2070048218020096

1. INTRODUCTION

An experimental study of fusion plasma involves the construction of multilevel radiation-gas-dynamic computational models that adequately describe the processes in the core of a pulsed fusion reactor. Thus, computational and theoretical methods are an important element in the process of developing the concept of magnetic confinement fusion (MCF) [1–3]. It should be recalled that an MCF system is a pulsed thermonuclear facility, in which a cylindrically or spherically symmetric fusion target placed in a seed (external) magnetic field is compressed (along with the seed's magnetic flow) by powerful laser beams or all kinds of shells, including gas, liquid, and metal drums, the plasma liners formed by the fusion of high-speed plasma jets, etc. It should be noted here that in [3] the authors present the initial estimates of the thermophysical plasma parameters, energy consumption for the electromagnetic field compression, and the work of vortical currents. Obviously, in this case, the developed mathematical models and methods of computational plasmodynamics of the MCF targets necessarily require verification based on a comparison with the reliable calculation data and the data of the physical experiments.

2. PROBLEM STATEMENT

In the general case, the object of MCF research is the spatial flows of the emitting target plasma in the presence of heat and mass transfer, electromagnetic fields, and nuclear reactions. The solution of these problems involves the use of complex plasmodynamic mathematical models that describe the processes taking place in fusion plasma, as well as the creation of highly precise numerical methods for their solution that enable adequate numerical simulation. At the same time, the initial study of the basic physical laws inherent in MCF should preferably be based on a system of simplified one-dimensional mathematical models.

2.1. Mathematical Model

We will describe the mathematical model simulating the compression process of MCF thermonuclear targets for a centrally symmetric coordinate system. The mathematical model of MCF targets presented in this work is based on the one-dimensional equations of radiation plasmodynamics, i.e., the system of Euler equations (1), the transfer equation of the broadband self-radiation (2), magnetic induction equation (3), laser radiation transfer equation, methods for calculating the equations of the state of matter, and

the absorption coefficients of laser radiation; and it determines the conditions for the occurrence and flow of a self-sustained thermonuclear fusion reaction:

$$\begin{gathered}\frac{\partial \rho}{\partial t}+\frac{1}{r^{(\nu-1)}}\frac{\partial\left(r^{(\nu-1)}\rho u\right)}{\partial r}=F_{\rho},\quad F_{\rho}=-\rho u\frac{(\nu-1)}{r},\\ \frac{\partial(\rho u)}{\partial t}+\frac{1}{r^{(\nu-1)}}\frac{\partial\left(r^{(\nu-1)}(\rho u^2+P)\right)}{\partial r}=F_{\rho u}+f_r,\quad F_{\rho u}=-(\rho u^2-P)\frac{(\nu-1)}{r},\quad f_r=\frac{1}{c}[\mathbf{j}\times\mathbf{H}]_r,\\ \frac{\partial(\rho E)}{\partial t}+\frac{1}{r^{(\nu-1)}}\frac{\partial\left(r^{(\nu-1)}(\rho Eu+Pu+q_{\Sigma})\right)}{\partial r}=F_E+q_r+Q^e_{Fus},\quad q_r=j_rE_r,\quad q_{\Sigma}=q_e+q_i+q_{\text{las}},\\ F_E=-(\rho Eu+Pu)\frac{(\nu-1)}{r},\quad P=P_e+P_i,\end{gathered}\tag{1}$$

where t is the time, r stands for the radial coordinate, ρ is the density, u denotes the velocity along the coordinate r, $P=P(\rho,\varepsilon)$ is the static pressure, ε is the specific internal energy, $E=(\varepsilon+u^2/2)$ denotes the total energy of gas flow, $\mathbf{F}=(F_{\rho},F_{\rho u},F_E)$ designates the sources vector in the orthogonal coordinate system, F_{ρ} stands for the mass flow density, $F_{\rho u}$ is the momentum flux density, F_E is the energy flux density, q and q_{ν} are the total and spectral radiation flux, T_e and T_i are the temperatures of the plasma electrons and ions ($T=T_e=T_i$), χ_{ν} is the spectral absorption coefficient, f_r is the electromagnetic force, q_r is the energy inflow from the electromagnetic field, $q_e=-\lambda_e\operatorname{grad}T_e$, $q_i=-\lambda_i\operatorname{grad}T_i$, q_{las} is the laser radiation flux, λ_e and λ_i are the thermal conductivity coefficients of the electrons and ions, j_r is the current density, $\mathbf{H}(r)$ is the magnetic induction vector, P_e denotes the electron pressure, P_i is the ion pressure, and the index $\nu=(1,2)$ corresponds to cases of plane and axial symmetry.

The contribution of the local (thermonuclear) energy release Q^e_{Fus} to the electronic component of the plasma due to the energy transfer to electrons from thermonuclear α-particles can be determined by the approximate formula [4], i.e.,

$$Q^e_{Fus}=8.483\times10^{29}\rho^2\frac{(1+0.232T_i^{3/4})\exp(-20/T_i^{1/3})}{T_i^{2/3}\sqrt{1+9.41\times10^{-5}T_i^{13/4}}}\ \ [\text{Erg}/(\text{cm}^3\,\text{s})],$$

where the temperature is set in keV and the density is set in g/cm^3.

The transfer of the broadband radiation can be considered using a multigroup diffusion approximation, the equations of which have the following form [5]:

$$\frac{1}{r^n}\frac{d(r^nq_{\nu})}{dr}+\chi_{\nu}cU_{\nu}=\chi_{\nu}4\sigma T^4,\quad \frac{c}{3}\frac{dU_{\nu}}{dr}+\chi_{\nu}q_{\nu}=0,\tag{2}$$

where q_{ν} and U_{ν} are the spectral flux and volume density of the broadband radiation, c is the velocity of light, ν denotes the frequency group number, χ_{ν} stands for the spectral absorption coefficient, $n=0$ is a plane layer, and $n=1$ is an infinite one-dimensional cylinder. Here, the quantity q_{ν} is understood as the radiation flux in the direction of the axis r.

The magnetic induction equation, which takes into account the continuity equation for the density ρ and the conservation law of the form $\operatorname{div}(\mathbf{H})=0$, are written as follows [6]:

$$\frac{\partial(B_z/\rho)}{\partial t}+\frac{1}{\mu J}\frac{\partial J(\nu B_z/\rho)}{\partial r}=\frac{c^2}{4\pi\mu\rho Jr}\frac{\partial}{\partial r}\left(\frac{Jr}{\sigma}\frac{\partial B_z}{\partial r}\right).\tag{3}$$

Electroconductivity is determined by Spitzer's formula [7] with allowance for the possible plasma magnetization, i.e.,

$$\sigma(z)=12.06\times10^{13}\frac{T^{3/2}}{\ln\Lambda\sum\limits_i n_iz_i^2}\frac{1}{1+(\Omega_e\tau_e)^2}\ \ [1/\text{s}]$$

where n_e and n_i are the concentrations of electrons and ions (cm^{-3}), z_i is the average ion charge, $\Omega_e=e|\mathbf{B}|/m_ec$ denotes the electron gyrofrequency, and m_e and M_i are the electron and ion masses, respectively.

The coefficients of electronic and ionic thermal conductivity $\lambda_{e,i}$ in the case of a magnetized plasma can be calculated using formulas [8].

The parameters of the laser radiation along the axis r are obtained based on the solution of the laser radiation transfer equation

$$\frac{dq_{\text{las}}}{dz} - \chi_\omega q_{\text{las}} = 0. \tag{4}$$

In this case, the absorption coefficient χ_ω of the laser radiation is determined using the mechanism of continual absorption inverse to the mechanism of bremsstrahlung of electrons in conditions of local thermodynamic equilibrium (LTE):

$$\chi_\omega = \begin{cases} \dfrac{4.97 g Z_i^2 n_i^{\Sigma} n_e^{\Sigma}}{n_c^2 \lambda^2 (kT_e)^{3/2}} \dfrac{1}{\sqrt{1 - n_e/n_c}}, & n_e < n_c, \\ \infty, & n_e \geq n_c, \end{cases}$$

where λ is the wavelength of laser radiation (μm), kT_e is the electron temperature (keV), and g is the Gaunt factor [8, 9].

The equations of the thermodynamic $e(T,\rho), P(T,\rho)$ and optical $\chi_i(T, \rho)$ parameters of the working media are calculated within the LTE approximation using the computer system ASTEROID developed by S.T. Surzhikov, a corresponding member of the Russian Academy of Sciences [10, 11], the Thomas–Fermi model with quantum and exchange corrections [12, 13], and the mean charge model [14, 15].

2.2. Initial Conditions

The MCF computational domain and target consist of a central part of one and the same coaxial layer. They have a cylindrical shape and the initial parameters of the target and the surrounding medium are within the following range of values:

• The central part of the target (the radius of the nucleus $R_{\text{nucl}} = 0.05$ cm) is filled with a D-T mixture with the density $\rho = 5 \times 10^{-2}$ g/cm^3 and initial temperature $T = 297$ K. It is surrounded by a coaxial layer (the outer radius $R_c = 0.1$ cm) made of metal (Al) with the density $\rho = 2.7$ g/cm^3, and initial temperature $T = 297$ K.

• The outer radius of the computational domain is $r = l = 0.2$ cm. At the same time, the thermodynamic parameters of the external rarefied environment (consisting of Ar) are given by the following values: $T =$ 297 K and $\rho = 2.7 \times 10^{-3}$ g/cm^3.

The initial value of the seed magnetic field intensity $\mathbf{H}(r)$ in a rarefied environment is a fraction of a tesla. The spectral flux and volume density of broadband radiation q_ν and U_ν, and the laser radiation flux q_{las} for $r \in [0, \ell]$ at the initial time instant $t = 0$ are zero.

2.3. Boundary Conditions

The symmetry condition (on the symmetry axis) is imposed as the boundary condition for the system of Euler equations (1), and nondisturbing conditions are set on the outgoing flow from the computational domain on the external boundary: $\left.\dfrac{\partial^2 \mathbf{f}}{\partial r^2}\right|_{r=\ell} = 0$, where $\mathbf{f} = \{\rho, u, v, e\}$.

The boundary conditions for solving the magnetic induction equation (3) can be described as follows: on the symmetry axis, the symmetry condition is imposed, and at the outer boundary, $\partial \mathbf{H}(r)/\partial r = 0$.

The boundary conditions for the system of equations of the diffusion approximation (2) can be formulated as follows: on the outer boundary, the absence of radiation incident from the outside is specified and on the symmetry axis the symmetry condition is imposed. The calculation of the laser radiation (4) along the axis r must involve the corresponding boundary conditions, i.e., $q_{\text{las}}\big|_{r=\ell} = q_{\text{las}}^0 \exp[-(t/\tau)^2]$, $q_{\text{las}}\big|_{r=0} = 0$, where τ is the half-width of the laser pulse at the half-height.

3. COMPUTATIONAL ALGORITHM

The method for the numerical solution of one-dimensional equations of the plasma dynamics of MCF targets is based on the method of fractional steps, which in this case is the two-step technique [16]. At the first fractional step, the gas-dynamic processes are taken into account (these processes correspond to the hyperbolic part of the considered system of equations). The processes of radiation transfer and electromagnetic processes occurring in the MCF system's devices are considered at the second fractional step.

It should be noted that the above-mentioned systems of differential equations in variable time t are systems of first-order ordinary differential equations that can be resolved using a vector variant of the multistep Runge–Kutta method (in this paper we use the four-step version of the method [17], which has the 4th order of time approximation).

At the first fractional step, the divergent form of the Euler equations is employed. Here (for the fractional time step $t \in [t, t + \Delta t/2]$), a nonlinear quasi-monotonic compact-polynomial difference scheme of higher order of accuracy is applied, i.e.,

$$\frac{\partial \mathbf{U}_i}{\partial t} + \frac{F(\mathbf{U}_{i+1/2}) - F(\mathbf{U}_{i-1/2})}{\Delta_\xi} = \mathbf{F}_2, \quad \Delta_\xi = \left[\xi_{i-1/2} - \xi_i, \xi_{i+1/2} - \xi_i\right].$$

The gasdynamic parameters U_i^{n+1} and U_i^n refer to the centers of the computational cells, while the fluxes $F_{i\pm1/2}^n$ must be determined on the surface of these cells. At the same time, in order to increase the approximation order of the difference scheme, it is necessary to restore the gas dynamic parameters $Y_{i\pm1/2}^{R,L}, Y_i^{R,L}$ to the right (index R) and to the left (index L) of the boundaries of the computational cells. Then any reconstructed function, $Y(x), [x = \{\xi\}]\ \xi \in [-\Delta_\xi/2, \Delta_\xi/2]$, is represented by piecewise polynomial distributions of the following form (in this case, we use a nonlinear quasi-monotonic compact polynomial difference scheme of a higher order of accuracy):

$$Y(\xi) = F_i^n(\xi) = Y_i + \phi(Y_i)\left(\frac{\partial Y}{\partial \xi}\right)_i [\xi - \xi_i] + \frac{\phi(Y_i)}{2!}\left(\frac{\partial^2 Y}{\partial \xi^2}\right)_i [\xi - \xi_i]^2$$

$$+ a_i[\xi - \xi_i]^3 + b_i[\xi - \xi_i]^4 + c_i[\xi - \xi_i]^5 + d_i[\xi - \xi_i]^6 + e_i[\xi - \xi_i]^7,$$

where $\phi(Y)$ is a limiter function [18]

$$\phi(Y_i) = \min\left(1, \frac{|Y_i - \max(Y_k)|}{\left|Y_i - \max\left(Y_{k-1/2}, Y_{k+1/2}\right)\right|}, \frac{|Y_i - \min(Y_k)|}{\left|Y_i - \min\left(Y_{k-1/2}, Y_{k+1/2}\right)\right|}\right),$$

where $k = i - 2, i - 1, i + 1, i + 2$.

The function $Y(x)$ satisfies the conditions of smooth conjugation, i.e.,

$$F_i^n(\xi_{i-1}) = Y_{i-1}^n, \quad F_i^n(\xi_{i+1}) = Y_{i+1}^n, \quad \frac{dF_i^n(\xi_{i-1})}{d\xi} = Y_{\xi,i-1}^n, \quad \frac{dF_i^n(\xi_{i+1})}{d\xi} = Y_{\xi,i+1}^n,$$

and of conservation:

$$\frac{1}{\Delta_\xi}\int_{-\Delta_\xi/2}^{+\Delta_\xi/2} Y_i^n(\xi)d\xi = Y(\xi_i).$$

The above-mentioned conditions of smooth conjugation can be formulated as a system of linear algebraic equations

$$A\mathbf{Z}_i = \mathbf{F}_i, \quad \mathbf{Z}_i = (a_i, b_i, c_i, d_i, e_i)^{\mathrm{T}}, \quad \mathbf{F}_i = (F_1, F_2, F_3, F_4, F_5)^{\mathrm{T}},$$

$$A = \begin{pmatrix} -\Delta_\xi^3 & \Delta_\xi^4 & -\Delta_\xi^5 & \Delta_\xi^6 & -\Delta_\xi^7 \\ 3\Delta_\xi^2 & -4\Delta_\xi^3 & 5\Delta_\xi^4 & -6\Delta_\xi^5 & 7\Delta_\xi^6 \\ \Delta_\xi^3 & \Delta_\xi^4 & \Delta_\xi^5 & \Delta_\xi^6 & \Delta_\xi^7 \\ 3\Delta_\xi^2 & 4\Delta_\xi^3 & 5\Delta_\xi^4 & 6\Delta_\xi^5 & 7\Delta_\xi^6 \\ 0 & \frac{1}{5}(\Delta_\xi/2)^4 & 0 & \frac{1}{7}(\Delta_\xi/2)^6 & 0 \end{pmatrix},$$

$$F_1 = Y_{i-1}^n - Y_i + \phi(Y_i)\left(\frac{\partial Y}{\partial \xi}\right)_i \Delta_\xi - \frac{\phi(Y_i)}{2!}\left(\frac{\partial^2 Y}{\partial \xi^2}\right)_i \Delta_\xi^2, \quad F_2 = Y_{\xi,i-1}^n - \phi(Y_i)\left(\frac{\partial Y}{\partial \xi}\right)_i + \phi(Y_i)\left(\frac{\partial^2 Y}{\partial \xi^2}\right)_i \Delta_\xi,$$

$$F_3 = Y_{i+1}^n - Y_i - \phi(Y_i)\left(\frac{\partial Y}{\partial \xi}\right)_i \Delta_\xi - \frac{\phi(Y_i)}{2!}\left(\frac{\partial^2 Y}{\partial \xi^2}\right)_i \Delta_\xi^2, \quad F_4 = Y_{\xi,i+1}^n - \phi(Y_i)\left(\frac{\partial Y}{\partial \xi}\right)_i - \phi(Y_i)\left(\frac{\partial^2 Y}{\partial \xi^2}\right)_i \Delta_\xi,$$

$$F_5 = -\frac{\phi(Y_i)}{3!}\left(\frac{\partial^2 Y}{\partial \xi^2}\right)_i \left[\frac{\Delta_\xi}{2}\right]^2.$$

The matrix A here is fixed, which implies that the inverse matrix A^{-1} is also fixed and can be found before carrying out the basic calculations.

The spatial derivatives $(\partial Y/\partial \xi)_{i,j}$ in the piecewise polynomial distributions $Y(\xi)$ are calculated as follows: first, for the discrete function Y_i, we obtain the approximate value F_i of the first partial derivative with respect to the spatial variable ξ with the eighth order of accuracy.

To do this, in each cell with number i, for each reconstructed quantity $Y_{i,j}$, we calculate the nonmonotonicity index $\mathrm{Ind}(Y)$, i.e.,

$$\mathrm{Ind}(Y)_i = \frac{\frac{1}{12}\left|-Y_{i+2,j} + 16Y_{i+1,j} - 30Y_{i,j} + 16Y_{i-1,j} - Y_{i-2,j}\right|}{\left(\frac{1}{2}\left|-Y_{i+2,j} + 4Y_{i+1,j} - 3Y_{i,j}\right| + \frac{1}{2}\left|3Y_{i,j} - 4Y_{i-1,j} + Y_{i-2,j}\right| + \theta\right)},$$

where the quantity θ is a small parameter.

Next we find the first derivative f with respect to the variable ξ by the usual approximation formula of the second order of accuracy and impose its monotonic constraint on the grid

$$\overline{\mathrm{Ind}}(Y)_i = 1\mathrm{Ind}(Y)_i + 2\left[1 - \mathrm{Ind}(Y)_i\right], \quad f_i = \frac{Y_{i+1} - Y_{i-1}}{2\Delta_\xi} + O\left(\Delta_\xi^2\right),$$

$$\tilde{f}_i = \mathrm{sgn}(Y_{i+1} - Y_{i-1}) \min\left(\overline{\mathrm{Ind}}(Y)_{i+2}|f_{i+2}|, \overline{\mathrm{Ind}}(Y)_{i+1}|f_{i+1}|, |f_i|, \overline{\mathrm{Ind}}(Y)_{i-1}|f_{i-1}|, \overline{\mathrm{Ind}}(Y)_{i-2}|f_{i-2}|\right),$$

where Δ is the step of the 3D grid in the direction of ξ. Then the approximate monotonized value $\tilde{F}_i$ of the first partial derivative with respect to the spatial variables ξ with an approximation error at the level $F_i = \frac{\partial}{\partial \xi} + \frac{\Delta_\xi^6}{2100} + O(\Delta_\xi^8)$ can be found by solving a system of equations with a tridiagonal matrix

$$Q_i = \left(E + \Delta_2/30\right)\tilde{f}_i, \quad \widetilde{F_i} = \left\{\left(E + \Delta_2/6\right)^{-1} Q_i\right\}_i,$$

$$F_i = \mathrm{sgn}(Y_{i+1} - Y_{i-1}) \min\left(\overline{\mathrm{Ind}}(Y)_{i+2}\left|\tilde{F}_{i+2}\right|, \overline{\mathrm{Ind}}(Y)_{i+1}\left|\tilde{F}_{i+1}\right|, \left|\tilde{F}_{i+1}\right|, \overline{\mathrm{Ind}}(Y)_{i-1}\left|\tilde{F}_{i-1}\right|, \overline{\mathrm{Ind}}(Y)_{i-2}\left|\tilde{F}_{i-2}\right|\right),$$

where $\Delta_0 f_i = f_{i+1} - f_{i-1}$, $\Delta_2 f_i = f_{i+1} - 2f_i + f_{i-1}$, and E is the unit operator. This formula is a symmetric finite difference of the sixth order of accuracy [19].

This method for calculating the first derivative F_i is used to define the boundary conditions on obtaining the approximate monotonized value $\tilde{F}_i$ of the first partial derivative with respect to the spatial variables

ξ with the approximation error at the level $F_i = \partial/\partial\xi + \Delta_\xi^8/44100 + O(\Delta_\xi^{10})$. In this case, the calculations should be carried out as follows (based on solving a system of equations with a five-diagonal matrix) [19]:

$$Q_i = \left(E + 5\Delta_2/42\right)\tilde{f}_i, \quad F_i = \left\{\left(E + 2\Delta_2/7 + \Delta_2^2/70\right)^{-1} Q_i\right\}_i.$$

Spatial derivatives of the second order $(\partial^2 Y/\partial\xi^2)_i$ are calculated with the eighth order of accuracy [20].

Next, using the reconstructed function $Y(\xi)$ we recover the gasdynamic parameters $Y_{i\pm1/2}^{R,L}, Y_i^{R,L}$ to the right (index R) and to the left (index L) of the boundaries of the computational cells. Then the antifusion correction of the reconstructed parameters $Y(\xi)$ is carried out $Y(\xi)$ at the edges of the cell $Y_{i\pm1/2}^{R,L}, Y_i^{R,L}$ [21].

It is known from the approximation theory of functions $Y(\xi)$ by a truncated Taylor series [22], that oscillations of the interpolated function can arise in the vicinity of discontinuities of the original function $Y(\xi)$ (and in the regions of large gradients of the solution). However, the function $Y(\xi)$ can be expanded in a series of a more general form (in the Bürmann–Lagrange series [23, 24]) in powers of some function $f(\xi - \xi_i)$. In this case, it is possible to select a function so as to reduce the amplitude of the parasitic oscillations of the numerical solution in the region $\ell_i \approx 1$.

Let the principal part of the reconstructed function $Y(x), [x = \{\xi\}]$, $\xi \in [-\Delta_\xi/2, \Delta_\xi/2]$, be an expansion into a series in powers (such a form of the function $f(x)$ adequately describes the behavior of the function $Y(\xi)$ near discontinuities of the first kind) of $f(x) = \Delta_\xi \tanh((\beta/\Delta_\xi)(\xi - \xi_i))$, $\beta = 4\mathrm{Ind}(Y) + 6(1 - \mathrm{Ind}(Y))$ by means of the Bürmann–Lagrange expansions [25, 26]. Then the reconstructed function $Y(\xi)$ can be written as

$$Y(\xi) = F_i^n(\xi) = Y_i + \phi(Y_i)\left\{f(\xi - \xi_i)p_1 + \frac{f^2(\xi - \xi_i)}{2!}p_2\right\}$$
$$+ a_i[\xi - \xi_i]^3 + b_i[\xi - \xi_i]^4 + c_i[\xi - \xi_i]^5 + d_i[\xi - \xi_i]^6 + e_i[\xi - \xi_i]^7,$$
$$p_1 = \left(\frac{\partial Y}{\partial\xi}\right)_i \Big/ \left(\frac{\partial f}{\partial\xi}\right)_i, \quad p_2 = \left(\frac{\partial^2 Y}{\partial\xi^2}\right)_i \Big/ 2\left(\frac{\partial f}{\partial\xi}\right)_i^2 - \left(\frac{\partial Y}{\partial\xi}\right)_i \left(\frac{\partial^2 f}{\partial\xi^2}\right)_i \Big/ 2\left(\frac{\partial f}{\partial\xi}\right)_i^3,$$

where p_1 and p_2 are the first coefficients of the expansion of the function $Y(\xi)$ in the truncated Bürmann–Lagrange series [23, 24]. It should also be noted [25] that under the condition $f(\xi) = \xi$ the coefficients p_1 and p_2 change into the usual Taylor series.

As before, for the reconstructed function $Y(\xi)$, the conditions of smooth conjugation and balance can be formulated as a system of linear algebraic equations (it should be noted that in this case the matrix A remains unchanged)

$$A\mathbf{Z}_i = \mathbf{F}_i, \quad \mathbf{Z}_i = (a_i, b_i, c_i, d_i, e_i)^{\mathrm{T}}, \quad \mathbf{F}_i = (F_1, F_2, F_3, F_4, F_5)^{\mathrm{T}},$$
$$F_1 = Y_{i-1}^n - Y_i - \phi(Y_i)\left\{-f(\Delta_\xi)p_1 + \frac{f^2(\Delta_\xi)}{2!}p_2\right\}, \quad F_2 = Y_{\xi,i-1}^n - \phi(Y_i)\left\{p_1 - f(\Delta_\xi)p_2\right\}\left(\frac{\partial f}{\partial\xi}\right)_{\Delta_\xi},$$
$$F_3 = Y_{i+1}^n - Y_i - \phi(Y_i)\left\{f(\Delta_\xi)p_1 + \frac{f^2(\Delta_\xi)}{2!}p_2\right\}, \quad F_4 = Y_{\xi,i+1}^n - \phi(Y_i)\left\{p_1 + f(\Delta_\xi)p_2\right\}\left(\frac{\partial f}{\partial\xi}\right)_{\Delta_\xi},$$
$$F_5 = -4\phi(Y_i)p_2\left(1 - \frac{2}{\beta}\tanh\left(\frac{\beta}{2}\right)\right)\left[\frac{\Delta_\xi}{2}\right]^2, \quad f(x) = \Delta_\xi \tanh\left(\frac{\beta}{\Delta_\xi}(\xi - \xi_i)\right).$$

It is clear from the above-mentioned relations that in a nonlinear quasi-monotonic compact-polynomial difference scheme, the distribution $Y(\xi)$ of gasdynamic parameters that are recoverable inside the computational cell $\xi \in [-\Delta_\xi/2, \Delta_\xi/2]$ is based on a polynomial of the 7th degree, and its main (nonsmooth) part near the discontinuities is singled out by a special technique (based on the Bürmann–Lagrange expansion) and is found using compact differences of the eighth order of accuracy [19, 20] (the first $(\partial Y/\partial\xi)_i$ and second derivatives $(\partial^2 Y/\partial\xi^2)_i$).

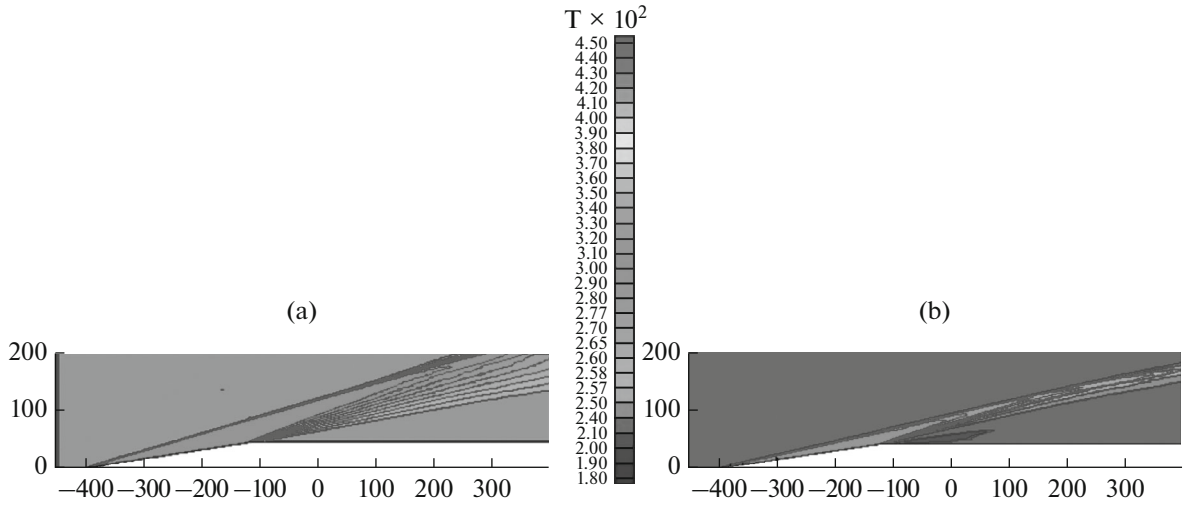

Fig. 1. Spatial distribution of temperature: (a) wedge conjugate to plate; (b) cone conjugate to cylinder.

The diffusion equation for the magnetic field and the heat equation were numerically solved using a compact difference scheme with increased accuracy [26]. The method for calculating the transfer of broadband radiation is considered based on the multigroup diffusion approximation [5]. The time step Δt necessary for integrating the compact-polynomial difference scheme presented above is chosen based on the condition for the fulfillment of the Courant–Friedrichs–Lewy stability criterion.

4. RESULTS AND DISCUSSION

The cogent analysis of the physical processes that may occur in the plasma of the MCF target requires verification of the proposed mathematical model and numerical methods by solving some test (model) problems.

The convective part of the computer model of MCF targets was tested on a one-dimensional version of the Riemann problem on the decay of an unstable discontinuity in a given configuration. A comparison of the exact and approximate solutions showed that the difference did not exceed one percent [27]. As additional test verification calculations, we considered the air flow around a wedge, which is conjugate to a plate (Fig. 1a), and around a cone (Fig. 1b) conjugate to a cylinder with the following parameters of the oncoming flow: pressure $P = 2060$ Pa, velocity $V = 1860$ m/s, temperature $T = 223$ K, and the Mach number $M_\infty = 6$. From [28] (for $M_\infty = 6$ and the angle of the wedge deviation from the symmetry plane $\upsilon = 8.7°$), it follows that the angle of inclination β of the shock wave is $\beta = 16°$ (in the calculation $\beta = 15.91°$, see Fig. 1a). Figure 1b shows similar results obtained for an air flow around a cone conjugate to a cylinder. At the same time, it follows from [28] (at $M_\infty = 6$ and $\upsilon = 8.7°$) that the inclination angle of the shock wave is $\beta = 12.9°$. This result is also in good agreement with the calculation performed (in calculation of $\beta = 12.85°$, see Fig. 1b).

The thermal part of the model was tested on some problems that admit exact analytical solutions such as heating a continuous medium [6] filling a flat semibounded space $r > 0$ with the heat flux through the fixed left boundary $r = 0$.

The presented group of calculations was carried out for the case of exposure to pulses of laser (Nd laser) radiation with the radiation flux density of about $q_{\text{las}} \approx 1\times10^{12}$–$1\times10^{14}$ [W/cm^2]. Now we briefly describe the obtained results graphically represented in Figs. 2–5. These results correspond to the following parameters of the mathematical model: $Q^e_{Fus} = 0$, the density of the laser radiation flux is $q_{\text{las}} = 2\times10^{14}$ [W/cm^2], and the half-width of the laser pulse is $\tau = 10$ [ns].

It follows from the performed calculations that the process of the laser compression of the MCF target located in an external magnetic field with respect to time t can be conditionally represented in three stages, i.e., the initial stage of the MCF target compression, the implosion stage of the MCF target, and the stage of the spreading of the plasma formation.

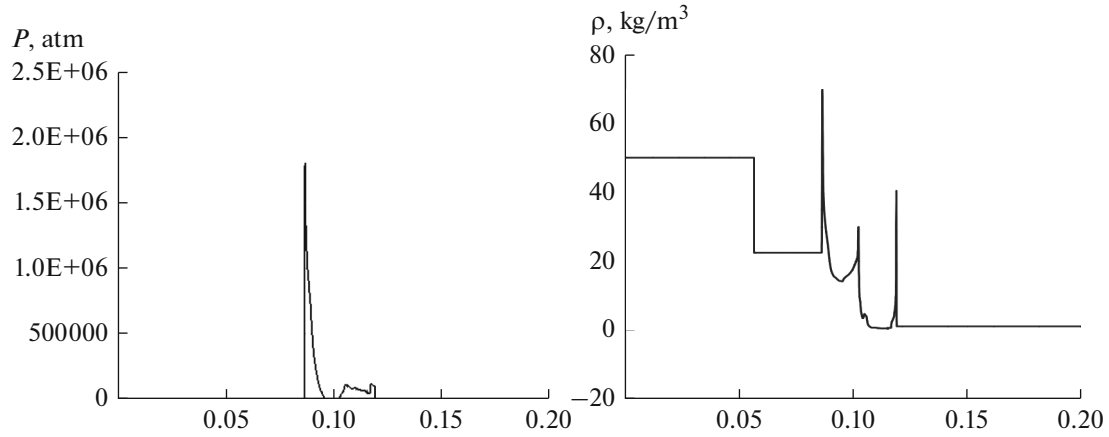

Fig. 2. Spatial distribution of pressure P and density ρ at time $t = 2.14$ ns.

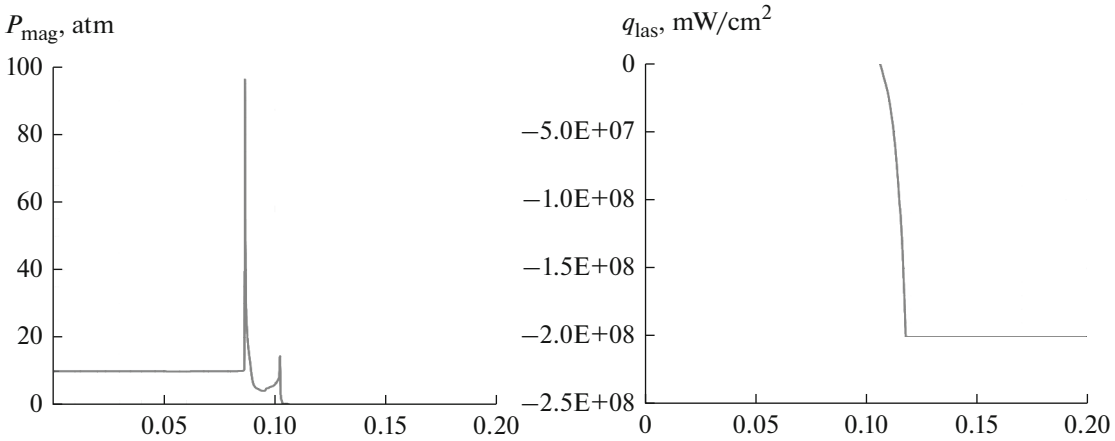

Fig. 3. Spatial distribution of magnetic pressure P_{mag} and flux of laser radiation q_{las} at time $t = 2.14$ ns.

Figures 2 and 3 show the distributions of the static P and magnetic P_{mag} pressure, density ρ, and the flux of the laser radiation q_{las}, which corresponds to the first initial compression stage ($t = 2.14$ ns) of the MCF target located in the external magnetic field. This stage corresponds to the autonomous propagation in the MCF target material of a system of two shock waves that arise from the release of the Joule energy

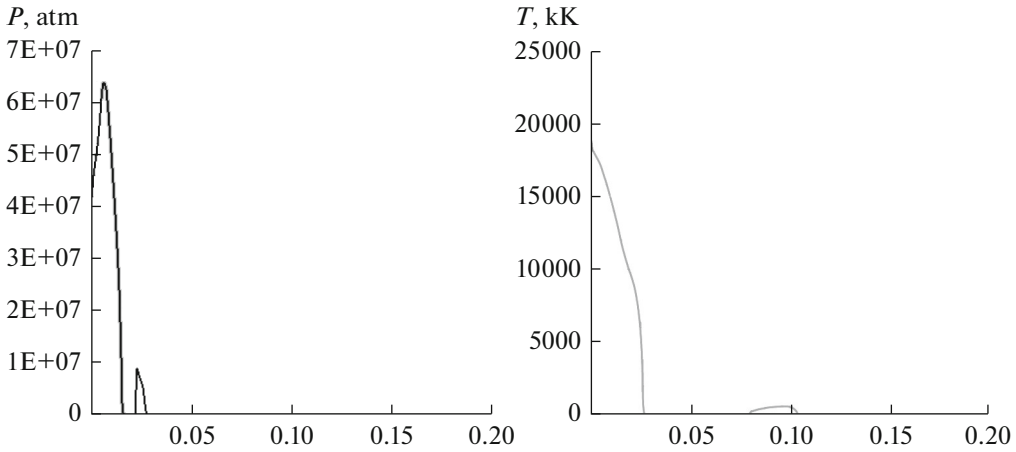

Fig. 4. Spatial distribution of pressure P and temperature T at time $t = 5.66$ ns.

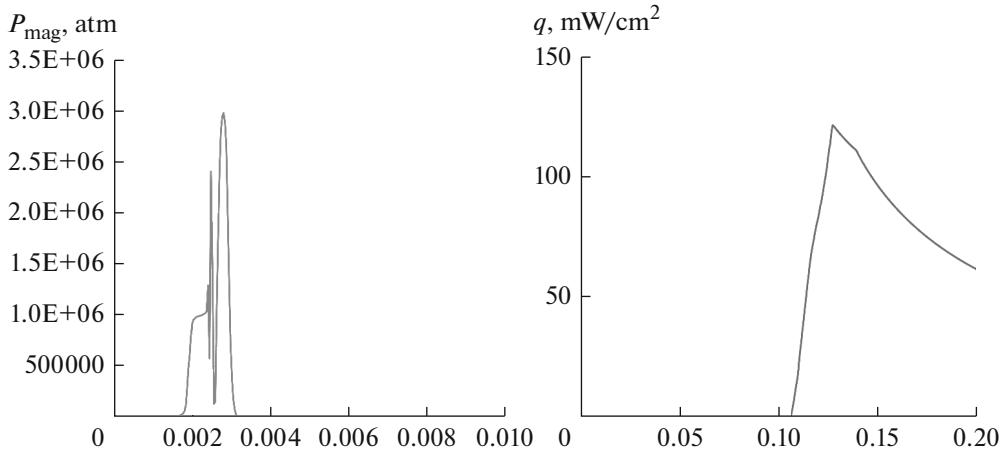

Fig. 5. Spatial distribution of magnetic pressure P_{mag} and total flux of intrinsic radiation of plasma q at time $t = 8.5$ ns.

and the absorption of the laser radiation energy in the plasma of the substance of the outer coaxial layer of the target (Fig. 3).

The graphs shown in Fig. 4 correspond to the implosion stage of the MCF target. The plasma-dynamic parameters of this stage are determined by the shock wave reflected from the symmetry axis and moving toward the outer boundary of the computational domain. At this stage, the bulk of the plasma formation is located near the origin of the coordinates. In this case, the maximum values of pressure and temperature of the MCF target plasma are observed near the symmetry axis of the target-chamber system of the reactor (Fig. 4).

Figure 5 shows the distributions of the magnetic pressure P_{mag} and the total flux q of the intrinsic radiation of the plasma formation ($t = 8.5$ ns).

ACKNOWLEDGMENTS

The work is supported by the Ministry of Education and Science of the Russian Federation (state order no. 13.5240.2017/BCh).

REFERENCES

1. O. G. Ol'khovskaya, V. A. Gasilov, M. M. Basko, et al., "Calculation of output power and X-ray spectrum of Z-pinches based on multiwire arrays," Math. Models Comput. Simul. **8**, 422–437 (2016).
2. S. V. Ryzhkov, "Current status, problems and prospects of thermonuclear facilities based on the magneto-inertial confinement of hot plasma," Bull. Russ. Acad. Sci.: Phys. **78**, 456–461 (2014).
3. V. V. Kuzenov and P. A. Frolko, "Standard and combined effects in the concept of magneto-inertial fusion," Applied Physics, No. 2, 21–27 (2015).
4. B. N. Kozlov, "Thermonuclear reaction rates," J. Nucl. Energy, Part C: Plasma Phys., Accel., Thermonucl. Res. **4**, 445 (1962).
5. B. N. Chetverushkin, *Mathematical Modeling of Problems in the Dynamics of Radiating Gas* (Nauka, Moscow, 1985) [in Russian].
6. A. A. Samarskii and Yu. P. Popov, *Differential Methods of Solving Problems of Gas Dynamics* (Editorial URSS, Moscow, 2009) [in Russian].
7. V. F. Diachenko and V. S. Imshennik, "To the magnetic hydrodynamical theory of pinch-effect in high temperature dense plasma," in *Problems of Plasma Theory* (Moscow, Atomizdat, 1967), No. 5, pp. 394–438 [in Russian].
8. S. I. Braginskii, "Transport phenomena in plasma," in *Problems of Plasma Theory* (Atomizdat, Moscow, 1963), No. 1, pp. 183–272 [in Russian].
9. Ya. B. Zeldovich and Yu. P. Raizer, *Physics of Shock Waves and High-Temperature Hydrodynamic Phenomena* (Academic, New York, 1967; Nauka, Moscow, 1966).
10. S. T. Surzhikov, "Computing system for solving radiative gasdynamic problems of entry and re-entry space vehicles," in *Proceedings of the 1st International Workshop on Radiation of High Temperature Gases in Atmospheric Entry, 2003,* ESA-533, pp. 111–118.

11. S. T. Surzhikov, *Thermal Radiation of Gases and Plasma* (Mosk. Gos. Tekh. Univ. im. N. E. Baumana, Moscow, 2004) [in Russian]; S. T. Surzhikov, *Computational Physics of Electric Discharges in Gas Flows* (Walter de Gruyter, Berlin, 2013).
12. V. V. Kuzenov, S. V. Ryzhkov, and V. V. Shumaev, "Thermodynamic properties of magnetized plasma evaluated by Thomas-Fermi model," Appl. Phys., No. 3, 22–25 (2014).
13. V. V. Kuzenov, S. V. Ryzhkov, and V. V. Shumaev, "Application of Thomas-Fermi model to evaluation of thermodynamic properties of magnetized plasma," Probl. At. Sci. Technol., No. 1 (95), 97–99 (2015).
14. V. V. Kuzenov, A. I. Lebo, I. G. Lebo, and S. V. Ryzhkov, *Physico-Mathematical Models and Calculation Methods for Effect of High-Power Laser and Plasma Pulses on Condensed and Gaseous Media* (Mosk. Gos. Tekh. Univ. im. N. E. Baumana, Moscow, 2015) [in Russian].
15. V. V. Kuzenov and S. V. Ryzhkov, "Numerical modeling of magnetized plasma compressed by the laser beams and plasma jets," Probl. At. Sci. Technol., No. 1 (83), 12–14 (2013).
16. V. M. Kovenia and N. N. Yanenko, *Splitting Method in Gas Dynamics Problems* (Nauka, Moscow, 1981) [in Russian].
17. K. N. Volkov and V. N. Emelianov, *Large-Eddy Simulation of Turbulent Flows in the Calculations* (Fizmatlit, Moscow, 2008) [in Russian].
18. T. J. Barth, "On unstructured grids and solvers," in *Computational Fluid Dynamics,* Vol. 1990-03 of *Lecture Series* (Von Karman Inst. Fluid Dynamics, Sint-Genesius-Rode, Belgium, 1990).
19. A. D. Savel'ev, "High-order composite compact schemes for simulation of viscous gas flows," Comput. Math. Math. Phys. **47**, 1332–1346 (2007).
20. L. E. Dovgilovich and I. L. Sofronov, "On application of compact schemes for solving the wave equation," KIAM Preprint No. 84 (Keldysh Inst. Appl. Math. RAS, Moscow, 2008).
21. O. Bokanowski, S. Martin, R. Munos, and H. Zidani, "An anti-diffusive scheme for viability problems," Appl. Numer. Math. **56**, 1147–1162 (2006).
22. V. I. Pinchukov, "Modelling of unsteady flows for large time intervals on the base of implicit high order schemes," Mat. Model. **16** (8), 59–69 (2004).
23. M. Abramowitz and I. Stegun, *Handbook of Mathematical Functions: with Formulas, Graphs, and Mathematical Tables* (Natl. Bureau of Standards, New York, 1972).
24. M. A. Lavrent'ev and B. V. Shabat, *Methods of Complex Analysis* (Nauka, Moscow, 1973) [in Russian].
25. E. V. Vorozhtsov, "Application of Lagrange–Burmann expansions for the numerical integration of the inviscid gas equations," Vychisl. Metody Program. **12**, 348–361 (2011).
26. A. I. Tolstykh, *Compact Differential Schemes and their Application in Aerohydrodynamics Problems* (Nauka, Moscow, 1990) [in Russian]; A. I. Tolstykh, "Hybrid schemes with high-order multioperators for computing discontinuous solutions," Comput. Math. Math. Phys. **53**, 1303–1322 (2013).
27. V. V. Kuzenov, and S. V. Ryzhkov, "Developing a procedure for calculating physical processes in combined schemes of plasma magneto-inertial confinement," Bull. Russ. Acad. Sci.: Phys. **80**, 598–602 (2016).
28. N. Y. Fabrikant, *Aerodynamics, General Course* (Nauka, Moscow, 1964) [in Russian].

Translated by I. Pertsovskaya